NANO LETTERS

2007
Vol. 7, No. 3
647−651

Shape Control of Multivalent 3D Colloidal Particles via Interference Lithography

Ji-Hyun Jang, Chaitanya K. Ullal, Steven E. Kooi, CheongYang Koh, and Edwin L. Thomas*

Institute for Soldier Nanotechnologies, Department of Materials Science and Engineering, Massachusetts Institute of Technology, Cambridge, Massachusetts 02139

Received November 9, 2006; Revised Manuscript Received January 24, 2007

ABSTRACT

We present a new route for the fabrication of highly nonspherical complex multivalent submicron particles. This technique exploits the ability of holographic interference lithography to control geometrical elements such as symmetry and volume fraction in 3D lattices on the submicron scale. Colloidal particles with prescribed complex concave shapes are obtained by cleaving low volume fraction connected structures fabricated by interference lithography. Controlling which Wyckoff sites in the space group of the parent structure are connected assures specific "valencies" of the particles. Two types of particles, 2D "4-valent" and 3D "6-valent" particles are fabricated via this technique. In addition to being able to control multivalent particle shape, this technique has the potential to provide tight control over size, yield, and dispersity.

Self-assembly of "simple" spherical colloidal particles has applications in chemical sensors, biomaterials, and optical components as well as photonic crystals.[1−6] The use of anisotropic shaped particles as the constituent building blocks offers increased possibilities[7] not only from their inherent material properties but also from novel types of particle packing. Especially, polymer-based micro- or nanoparticles with specific size and shape have been widely used for drug delivery.[8,9] For example, viruses, one type of biological nanoparticle with specific point group symmetries and metallic nanoparticles, have been suggested as building blocks for supramoecular architectures as the nanosensors for rapid detection of clinically relevant viruses.[10] To date, most fabrication methods for nonspherical particles have involved the modification of spherical particles. Thus, prolate ellipsoids have been produced by heating and then deforming spherical particles embedded in a matrix, followed by cooling to retain the anisotropic shape.[11,12] Irradiation of spherical colloids containg azo units by polarized light has also produced particles with an aspect ratio of over 2.[13] Highly ordered polyhedra have been fabricated through compaction-sintering of colloidal spheres.[14,15] Precise shape control of colloidal particles has been demonstrated by the use of photolithography with 2D masks. However, this control is presently restricted to 2D or quasi-2D structures.[11,12,16,17] Interfacial tension between the particle and the solvent during the synthesis of colloidal particles in the liquid phase, such as in microfluidic channels, generally restricts the generation of particles to spheres or modified spheres with rounded edges.[11,12,18,19] Ellipsoidal particles have been recently produced via 2D phase mask interference lithography, but at present, this method does not offer much control over rational design for complex shapes.[20]

Here, we report the use of holographic interference lithography (HIL) as an easy and high-throughput fabrication method for creating complex polymer particles with controlled symmetry, size, and highly nonconvex shapes. HIL has already been demonstrated as a promising approach to the fabrication of large-area and periodic 3D structures on the submicrometer scale.[21,22] One possible advantage of the HIL method for fabrication of particles is that a particle suprastructure with a particular point group that is not easily or otherwise accessible can be created by the reassembly of blends of particles with prescribed shapes. This approach can give access to a wider range of structures with novel optical or mechanical properties. HIL involves the formation of a stationary spatial variation of intensity created by the interference of two or more beams of light. The pattern that emerges out of the intensity distribution is transferred to a light-sensitive medium, such as a photoresist, to yield structures. Importantly, by proper choice of beam parameters, one can control the geometrical elements and volume fraction of the structures.[23,24]

Our multivalent particles are fabricated by creating disconnected HIL structures in a negative photoresist. Manipulation of the experimental parameters of intensity, polarization, phase, and wave vectors of the interfering beams allows one to target specific space group structures. We use beams that result in a higher contrast in the light intensity distribution with regions of high intensity being concentrated in Wyckoff sites of low multiplicity and high symmetry.[25] The use of a

* Corresponding author. E-mail: elt@mit.edu. Telephone: 617-253-5931. Fax: 617-253-5859.

10.1021/nl0626277 CCC: $37.00
Published on Web 02/13/2007

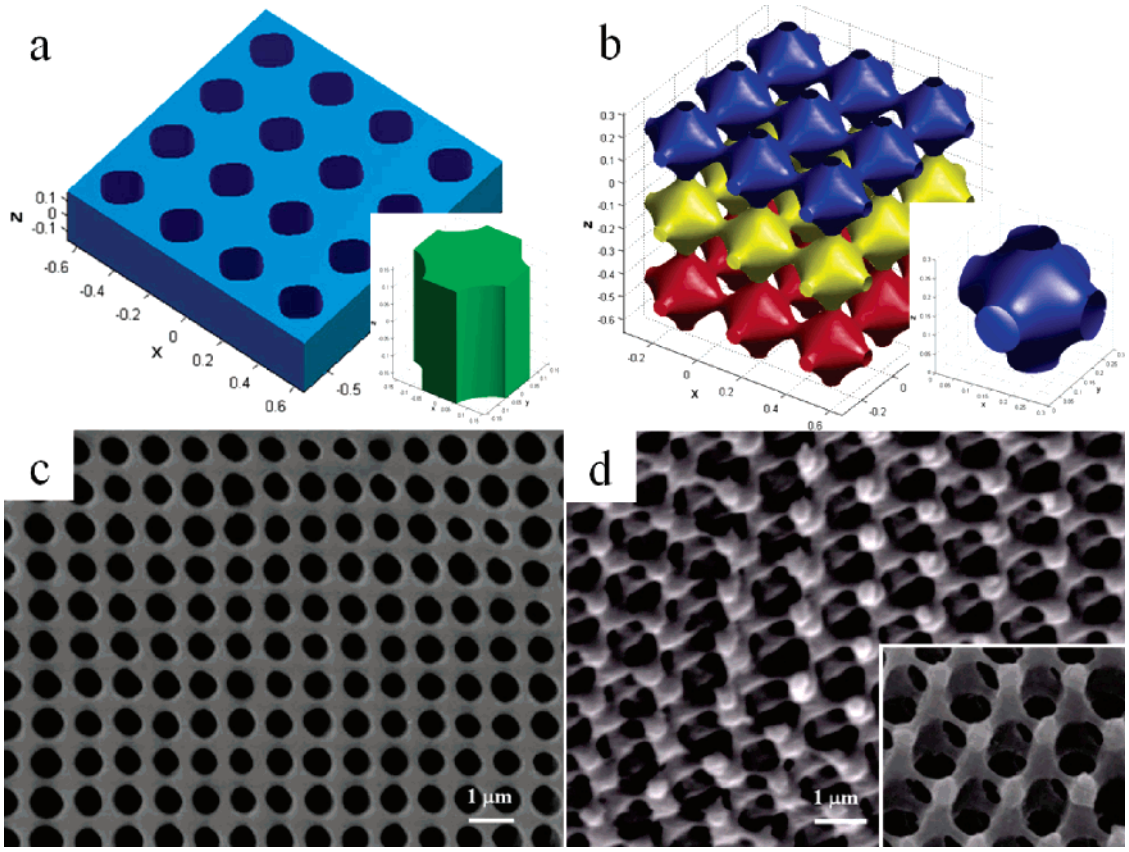

Figure 1. Comparison of theoretical and experimental structures. Perspective view of 4 × 4 2D square lattice (a) and 3 × 3 × 3 3D simple cubic lattice (b) based on the respective theoretical light intensity models. The lower right insets are the single unit cells of each structure; SEM images of the experimental 2D square (c) and 3D simple cubic (d) structures fabricated in SU8. The lower inset of (d) is a magnified tilted SEM image viewed along the ⟨111⟩ direction.

negative photoresist implies a high cross-link density of insoluble polymer in these regions. The valency of the resultant particles is determined by the connectivity of these Wyckoff sites and the process by which they become disconnected. To disconnect the structure, the thickness and cross-link density of the connecting arms is reduced by decreasing the exposure and by subsequent strong development. The particles can be separated either by chemical etching with O_2 plasma or UV/ozonolysis or by mechanical forces, for example, from the expansion due to the freezing of water in the continuous matrix region.

As a proof of concept, we demonstrate the fabrication of two types of concave multivalent polymer particles, 4-valent particles from a parent simple square lattice, and 6-valent particles from a parent simple cubic structure, via interference lithography. The light intensity distribution depends on the relative directions and polarizations of the interfering beams. The 2D simple square air hole lattice is made by double exposure with a 90° rotation of the sample in the plane of the sample between exposures. The directions and polarizations of the beams inside the photoresist are given by:

Simple square lattice

$$\vec{k}_0 = 2\pi/\lambda[0,0.316,0.949] \qquad \vec{E}_0 = [100]$$
$$\vec{k}_1 = 2\pi/\lambda[0,-0.316,0.949] \qquad \vec{E}_1 = [100]$$

The 3D bicontinuous polymer/air simple cubic structure is made by the superposition of six beams (coordinate system is oriented with each orthonormal axis parallel with each pair of coplanar beams, as shown in Figure S1b, Supporting Information):

$$\vec{k}_0 = 2\pi/\lambda[-0.970,-0.243,0] \qquad \vec{E}_0 = [001]$$
$$\vec{k}_1 = 2\pi/\lambda[-0.970,0.243,0] \qquad \vec{E}_1 = [001]$$
$$\vec{k}_2 = 2\pi/\lambda[0,-0.970,0.243] \qquad \vec{E}_2 = [100]$$
$$\vec{k}_3 = 2\pi/\lambda[0,-0.970,-0.243] \qquad \vec{E}_3 = [100]$$
$$\vec{k}_4 = 2\pi/\lambda[-0.243,0,-0.970] \qquad \vec{E}_4 = [010]$$
$$\vec{k}_5 = 2\pi/\lambda[0.243\ 0\ -0.970] \qquad \vec{E}_5 = [010]$$

where $\vec{k}_i$ and $\vec{E}_i$ are the wave vector and polarizations of the ith beam, respectively, and λ is the propagating wavelength of the beam in the photoresist. Perspective views of the targeted 2D square and the 3D simple cubic bicontinuous parent structures are shown in Figure 1a and 1b. The motif occupying the high-symmetry Wyckoff sites in each structure is shown in the single unit cell in the insets. SEM images of the corresponding long-range ordered polymer lattices are shown in Figure 1c and 1d. The 2D periodic square structure has plane group $p4$ mm symmetry, the high cross-link density

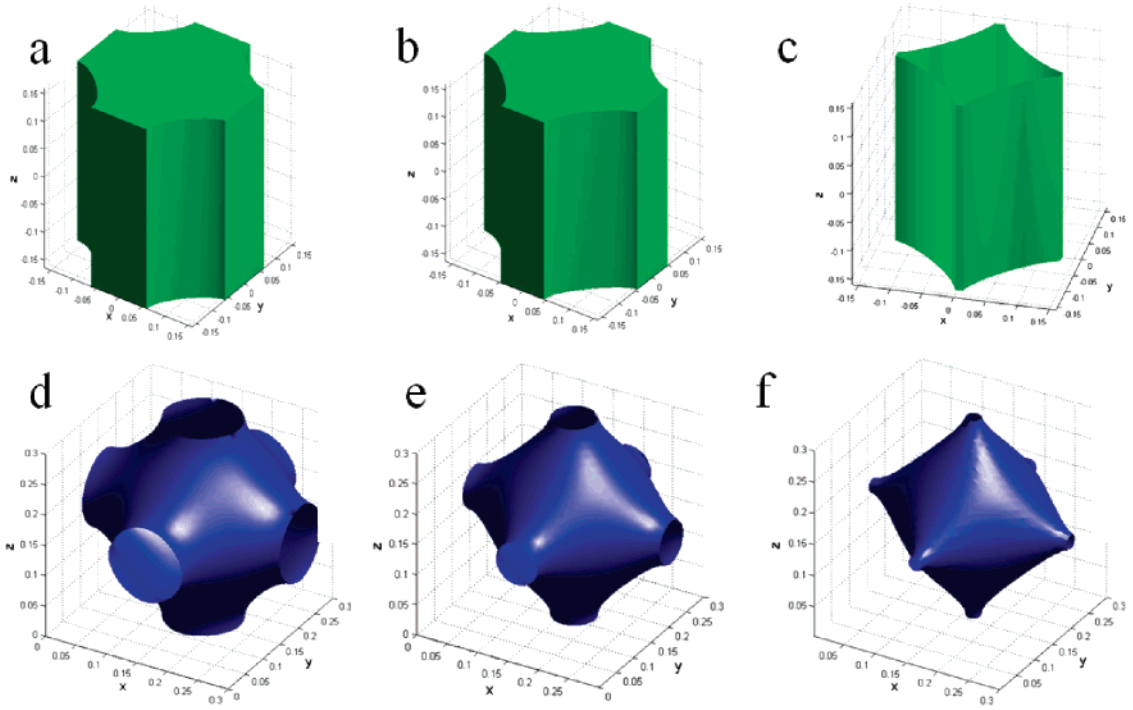

Figure 2. Theoretical modeling of pinch off structures. Single unit cells of square (a) and simple cubic (d) structures having 40% and 35% volume fraction. Single unit cells of square (b) and simple cubic structure (e) with 85% and 75% of light intensity of (a) and (d), respectively. Single unit cells of square (c) and simple cubic (f) particles formed after isotropic etching of (b) and (e) by strong solvent.

nodes occupy Wyckoff site 1a and are 4-connected alongthe ⟨10⟩ directions. The 3D periodic simple cubic structure is a member of the Schwarz P surface level set family (space group $Pm\bar{3}m$).[25] The high cross-link density nodes occupy Wyckoff site 1a and are 6-connected along the ⟨100⟩ directions. Because of the manner in which the particles disconnect, the resultant colloidal particles have a line "valency" of 4 for the square lattice and a point "valency" of 6 for the simple cubic structure.

The HIL technique allows for easy control of volume fraction along iso-intensity surfaces through several experimental parameters, i.e., laser intensity, time of exposure, and chemistry of the photoresist platform. Figure 2 shows the variation in particle shape as a function of volume fraction assuming various iso-intensity contours and the effect of an isotropic etch on the 2D square and 3D simple cubic structures, respectively. The isointensity contour determines the threshold that separates the highly cross-linked insoluble and low cross-linked soluble material. Parts b and e of Figure 2 show particles achieved by lowering the light intensity and subsequent solvent removal of the low cross-linked regions. Continuously decreasing the volume fraction of the network structure via lowering the exposure will eventually pinch off the thin areas and yield disconnected particles. However, simply decreasing light intensity along isointensities results in a less pronounced effect of the "valency" and less concave shapes in the final particles (Figures S2 and S3 in Supporting Information).[20] To retain the pronounced nature of the "valency" and a strongly concave particle shape, after an initial exposure and development, an isotropic etch using a stronger solvent, followed by supercritical CO_2 drying to prevent distortion of the structure due to high surface tension forces,[12,13,18,19,26] can result in particles with the desired shape (see models in Figure 2c and f).

Finally, the particles can be fully disconnected at the thinnest part of the arms between neighboring nodes to obtain the discrete multivalent colloidal particles. O_2 plasma or UV-assisted ozonolysis can remove organic polymer selectively and isotropically in 3D structures.[27] Because the whole structure has very thin connections, O_2 plasma or UV/ozonolysis does not affect the final shape of the particle, but only decreases the size of the polymer particle by 2−3%. Further, because this is a dry process, surface tension forces cannot distort the particles.

Figure 3 shows the SEM images of the experimental structures after the two steps. Figure 3a (for the square structure) and Figure 3b (for the simple cubic structure) are secondary electron images of the low volume fraction structures after dissolution of the lightly cross-linked and uncross-linked regions in the photoresist material by wet development in stronger solvent such as *N*-methyl-2-pyrrolidone (NMP), followed by supercritical CO_2 drying. The final individual polymer particles with specific symmetry after UV/ozonolysis are shown in Figure 3c (for the square structure) and Figure 3d (for the simple cubic structure). The polymer particles fabricated here closely resemble the theoretically computed structures displayed in the insets, confirming that the transfer of the light intensity pattern into the photoresist and the separation into discrete particles occurs with high fidelity.

An alternative to UV/ozonolysis to create separate particles is to infiltrate and crystallize water in the air regions of the

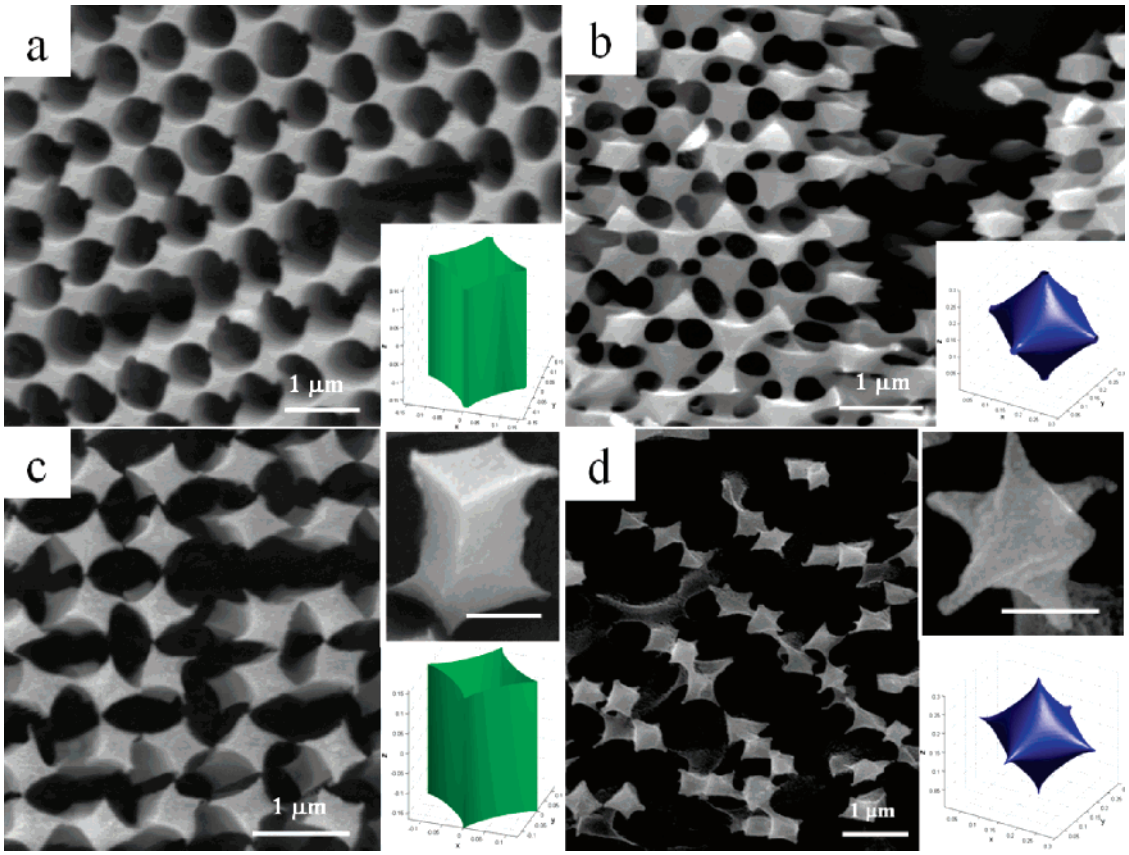

Figure 3. SEM images of 2D and 3D structures before and after UV/ozonolysis. (a and b) Lightly connected structures after first strong development followed by CO_2 supercritical drying. (c and d) Samples after UV/ozonolysis. Each lower inset shows the single unit cell with the calculated light intensity distributions corresponding to the SEM images. The upper insets in (c) and (d) are magnified individual "4-valent" and "6-valent" particles very similar to the theoretical model in the lower inset. The scale bars are 300 nm.

lightly cross-linked structure. After solidification of the water, the volume change on crystallization induces mechanical disconnection at the thin arms without any loss of particle shape. Freeze-drying the sample avoids passing through the liquid phase, and the final particles from this mechanical disconnect step are quite similar to the ones from the dry chemical etch approach.

In addition to control of particle valency and shape, HIL has other potential advantages related to the fabrication of colloids, viz. yield, control over dispersity, and size control. Large area 3D structures via HIL covering several square mm with submicrometer features have already been repeatedly demonstrated.[28] For a 6 in. wafer and 10 μm thick film containing 10 unit cells along the thickness direction, the yield from one exposure would be approximately 10^9 particles. Importantly, because the periodicity of the parent structure, and hence size of colloidal particles, is fixed by the wavelength and angle between the interfering beams, an extremely narrow size distribution of particles is readily achieved by this method. There is however a potential dispersity in the distribution of the particles in this method in the form of volume fraction. Volume fraction depends primarily on the volume fraction variation across the parent structure depending on the local intensity dose during the exposure of the photoresist. The use of a flat-top beam profile or expanded interfering beams would allow for a high yield of complex colloids with a tighter distribution both from a size and volume fraction perspective. Alternatively, by deliberate application of a spatially varying intensity profile, a tailored volume fraction distribution of particles may be obtained. Finally, changing the exposing wavelength can vary the size of the colloidal particles obtained. Limited control is also available by varying the angle between the beams. In some specific cases such as the 6-connected P surface particles, this control is greater as the parent structure is continuously size scalable with our IL setup configuration. In thicker films, volume fraction variation could also be introduced by chirp in the parent structure due to absorption in the photoresist film. This can be mitigated by using thinner films or photosensitizers dyes. Although at present our particles have only been fabricated in SU-8, our group has already fabricated 3D structures in poly(ethylene glycol) diacrylate with some modification. Therefore, multivalent particles from hydrogels that are responsive to pH or temperature are possible and currently being investigated. Additional types of multivalent particles from other than polymeric materials can be made by infiltration of the parent polymer template with, for example, a sol−gel to create polymer−ceramic composites, and after a suitable removal of the polymer and etch, interesting complex particles such as silica and Fe_2O_3, etc., can be created.

In summary, a facile, high-yield route for the fabrication of complex multivalent colloidal particles has been demonstrated. This technique exploits the ability of holographic

interference lithography to control network topology. Two types of concave particles, "4-valent" and "6-valent", were fabricated via this technique. In addition to being able to control shape and symmetry in the particles obtained, this technique has the potential to provide tight control over size and yield. Deposition of materials onto the surface of the cross-linked polymer lattice followed by the disconnection may introduce a different chemical functionality at the vertices of the particles, thereby providing the possibility of having particles with both anisotropic geometry and chemistry.

Acknowledgment. This work is supported in part by the Institute for Soldier Nanotechnologies of the U.S. Army Research Office and the National Science Foundation grant no. DMR-0414974.

Supporting Information Available: The interference lithographic setup, the detailed experimental procedures, and the modeling of isointensity distributions at various volume fractions. This material is available free of charge via the Internet at http://pubs.acs.org.

References

(1) Holtz, J. H.; Asher, S. A. *Nature* **1997**, *389*, 829.
(2) Miguez, H.; Meseguer, F.; Lopez, C.; Blanco, A.; Moya, J. S.; Requena, J.; Mifsud, A.; Fornes, V. *Adv. Mater.* **1998**, *10*, 480.
(3) Park, S. H.; Xia, Y. N. *Langmuir* **1999**, *15*, 266.
(4) Sanders, J. V.; Murray, M. J. *Nature* **1978**, *275*, 201.
(5) Velev, O. D.; Kaler, E. W. *Langmuir* **1999**, *15*, 3693.
(6) Yan, H. W.; Zhang, K.; Blanford, C. F.; Francis, L. F.; Stein, A. *Chem. Mater.* **2001**, *13*, 1374.
(7) van Blaaderen, A. *Nature* **2006**, *439*, 545.
(8) Chauvierre, C.; Labarre, D.; Couvreur, P.; Vauthier, C. *Pharm. Res.* **2003**, *20*, 1786.
(9) Vauthier, C.; Dubernet, C.; Fattal, E.; Pinto-Alphandary, H.; Couvreur, P. *Adv. Drug Delivery Rev.* **2003**, *55*, 519.
(10) Perez, J. M.; Simeone, F. J.; Saeki, Y.; Josephson, L.; Weissleder, R. *J. Am. Chem. Soc.* **2003**, *125*, 10192.
(11) Jiang, P.; Bertone, J. F.; Colvin, V. L. *Science* **2001**, *291*, 453.
(12) Xu, S. Q.; Nie, Z. H.; Seo, M.; Lewis, P.; Kumacheva, E.; Stone, H. A.; Garstecki, P.; Weibel, D. B.; Gitlin, I.; Whitesides, G. M. *Angew. Chem., Int. Ed.* **2005**, *44*, 724.
(13) Li, Y. B.; Tong, X. L.; He, Y. N.; Wang, X. G. *J. Am. Chem. Soc.* **2006**, *128*, 2220.
(14) Manoharan, V. N.; Elsesser, M. T.; Pine, D. J. *Science* **2003**, *301*, 483.
(15) Yin, Y. D.; Xia, Y. N. *Adv. Mater.* **2001**, *13*, 267.
(16) Dendukuri, D.; Pregibon, D. C.; Collins, J.; Hatton, T. A.; Doyle, P. S. *Nat. Mater.* **2006**, *5*, 365.
(17) Rolland, J. P.; Maynor, B. W.; Euliss, L. E.; Exner, A. E.; Denison, G. M.; DeSimone, J. M. *J. Am. Chem. Soc.* **2005**, *127*, 10096.
(18) Dendukuri, D.; Tsoi, K.; Hatton, T. A.; Doyle, P. S. *Langmuir* **2005**, *21*, 2113.
(19) Xia, Y. N.; Whitesides, G. M. *Angew. Chem., Int. Ed.* **1998**, *37*, 551.
(20) Jeon, S.; Malyarchuk, V.; Rogers, J. A.; Wiederrecht, G. P. *Opt. Express* **2006**, *14*, 2300.
(21) Campbell, M.; Sharp, D. N.; Harrison, M. T.; Denning, R. G.; Turberfield, A. J. *Nature* **2000**, *404*, 53.
(22) Moon, J. H.; Yang, S. *J. Macromol. Sci., Part C: Polym. Rev.* **2005**, *45*, 351.
(23) Toader, O.; Chan, T. Y. M.; John, S. *Phys. Rev. Lett.* **2004**, 92.
(24) Ullal, C. K.; Maldovan, M.; Wohlgemuth, M.; Thomas, E. L. *J. Opt. Soc. Am. A* **2003**, *20*, 948.
(25) Wohlgemuth, M.; Yufa, N.; Hoffman, J.; Thomas, L. E. *Macromolecules* **2001**, *34*, 6083.
(26) Yang, S.; Megens, M.; Aizenberg, J.; Wiltzius, P.; Chaikin, P. M.; Russel, W. B. *Chem. Mater.* **2002**, *14*, 2831.
(27) Chan, V. Z. H.; Hoffman, J.; Lee, V. Y.; Iatrou, H.; Avgeropoulos, A.; Hadjichristidis, N.; Miller, R. D.; Thomas, E. L. *Science* **1999**, *286*, 1716.
(28) Miklyaev, Y. V.; Meisel, D. C.; Blanco, A.; von Freymann, G.; Busch, K.; Koch, W.; Enkrich, C.; Deubel, M.; Wegener, M. *Appl. Phys. Lett.* **2003**, *82*, 1284.

NL0626277